



Amplification of optical Schrödinger cat states with an implementation protocol based on a frequency comb

Hongbin Song ^{*}

General Education Division and Shenzhen Key Lab of Semiconductor Lasers, The Chinese University of Hong Kong, Shenzhen, Guang Dong 518116, China

Guofeng Zhang [†]

Department of Applied Mathematics, The Hong Kong Polytechnic University, Kowloon 999077, Hong Kong, China and The Hong Kong Polytechnic University Shenzhen Research Institute, Shenzhen, Guang Dong 518057, China

Xiaoqiang Wang

Shenzhen Middle School No.18, Shenzhong Street, North Renmin Road, Shenzhen, Guang Dong 518024, China; Department of Applied Mathematics, The Hong Kong Polytechnic University, Kowloon 999077, Hong Kong, China; and The Hong Kong Polytechnic University Shenzhen Research Institute, Shenzhen, Guang Dong, 518057, China

Hidehiro Yonezawa [‡]

Centre for Quantum Computation and Communication Technology and School of Engineering and Information Technology, The University of New South Wales, Canberra, ACT 2600, Australia

Kaiquan Fan

School of Science and Engineering, The Chinese University of Hong Kong, Shenzhen 518116, China



(Received 4 November 2021; accepted 29 March 2022; published 20 April 2022)

We proposed and analyzed a scheme to generate large-size Schrödinger cat states based on linear operations of Fock states, squeezed vacuum states, and conditional measurements. By conducting conditional measurements via photon number detectors, two unbalanced small-amplitude Schrödinger kitten states combined by a beam splitter can be amplified to a large-size cat state with the same parity. According to simulation results, two Schrödinger odd kitten states with amplitudes of $|\beta| = 1.06$ and $|\beta| = 1.11$ generated from one-photon-subtracted 3 dB squeezed vacuum states, are amplified to an odd cat state of $|\beta| = 1.73$ with a fidelity of $F = 99\%$. A large-size Schrödinger odd cat state with $|\beta| = 2.51$ and $F = 97.30\%$ is predicted when 5.91 dB squeezed vacuum states are employed. According to the analysis on the impacts of experimental imperfections in practice, Schrödinger odd cat states of $|\beta| > 2$ are available. A feasible configuration based on a quantum frequency comb is developed to realize the large-size cat state generation scheme we proposed.

DOI: [10.1103/PhysRevA.105.043713](https://doi.org/10.1103/PhysRevA.105.043713)

I. INTRODUCTION

Optical Schrödinger cat states described as $|\beta\rangle + e^{i\phi} |-\beta\rangle$ for even cats and odd cats corresponding to $\phi = 0$ and $\phi = \pi$, respectively, are the superposition of two distinguishable coherent states $|\beta\rangle$ and $|-\beta\rangle$ with opposite phases, where $|\beta|$ describes the size of Schrödinger cat states [1]. Odd (even) cats are featured with odd (even) photon number distribution. Different from the mixture states, superposition states reveal the interference between superposed components, which play an important role in the verification of quantum nonlocality [2], quantum communication [3–5], continuous-variable quantum computation [6–10], and quantum metrology [11,12]. The one-photon subtracted squeezed vacuum

state is a standard method to generate Schrödinger cat states with small size, so-called Schrödinger kitten states [1]. Kitten states at baseband [13–16] and sidebands [17] have been generated, while the maximum amplitude of cat states generated with such method is limited as $|\beta| = 1.20$ to keep the fidelity as high as 99% [18,19]. Fidelity between an ideal cat state $|\phi\rangle$ and a generated pure state $|\psi\rangle$ is usually defined as $F(\phi, \psi) = |\langle\phi|\psi\rangle|^2$ [18,20] (the definition in the form of square root, i.e., $\langle\phi|\psi\rangle$ is also used in some references such as [19,21]), indicating the similarity of the generated state with an ideal cat state, which is an important quality measure of the cat state.

However, the overlap between two superposed coherent states in a Schrödinger cat state, i.e., $\langle\beta|-\beta\rangle = e^{-2|\beta|^2}$, is required to approach zero to effectively work as qubits in quantum information science, i.e., $|\beta| \geq 2$ [7]. Therefore, large-size Schrödinger cat states generation has attracted intense interest.

To create Schrödinger cat states with larger amplitudes, theoretical and experimental investigations on multiphoton

^{*} songhongbin@cuhk.edu.cn

[†] guofeng.zhang@polyu.edu.hk

[‡] h.yonezawa@unsw.edu.au

subtracted squeezed vacuum states were conducted [22–25]. An even cat state and an odd cat state of $|\beta| = 1.40$ and $F = 60\%$ as well as $|\beta| = 1.70$ and $F = 59\%$ were experimentally created by subtracting two and three photons from squeezed vacuum states [22,25], respectively. Based on a Fock state and homodyne detection, a squeezed even cat state [23] with $|\beta| = \sqrt{2.6} \approx 1.61$ was experimentally demonstrated [20]. An iterative scheme to amplify Schrödinger kitten states was proposed by conducting auxiliary-coherent-state-aided conditional measurement on two combined kitten states by a 50:50 beam splitter [18], from which a high-fidelity ($F \geq 99\%$) cat state with $|\beta| = 2.50$ was predicted with four iterative stages and inefficient photon detection. This approach was extended to a homodyne heralding scheme later, in which the conditional measurement with photon detectors and auxiliary coherent state was replaced with homodyne detection [26]. Two balanced Schrödinger odd kitten states with $|\beta| = 1.15$ squeezed by 1.74 dB were amplified to a Schrödinger even cat state of $|\beta| = 1.85$ squeezed by 3.04 dB with a fidelity of $F = 59.29\%$ (in the definition of $F = |\langle \phi | \psi \rangle|^2$) based on the homodyne heralding scheme [21], which was considered as the best experimental result till now [27]. A sequential photon catalysis scheme was proposed to generate large-size squeezed Schrödinger cat states [28], in which multistage photon catalyses are required to breed the cat state. Large-size Schrödinger cat states of $|\beta| > 2$ with a fidelity around $F = 99\%$ based on a two-mode nine-photon entangled state were predicted [29]. Recently, an optical cat state generation scheme based on the general photon subtraction of two squeezed vacua was reported with high generation rate, in which a large-size squeezed cat state of $|\beta| = \sqrt{10} \approx 3.16$ was predicted with a fidelity of $F = 99.7\%$ by subtracting ten photons from one mode of the two-mode squeezed vacuum states [27]. However, operations including multiphoton subtraction, iterative and sequential process significantly increase the complexity of the experimental setup in practice.

In this paper, we propose a scheme to generate large-size odd cat states based on linear operations of squeezed vacuum states and conditional measurements. Amplification of odd kitten states that keeps the same parity is realized. Schrödinger odd cat state of $|\beta| > 2$ is predicted with one-photon subtraction through a single run. We also develop a quantum-frequency-comb-based protocol to realize the scheme.

The paper is organized as follows. In Sec. II, a general model for l -added-and- k -subtracted squeezed vacuum states is introduced based on tensor operation. In Sec. III, an effective approach to producing large-size Schrödinger cat states is developed. The impacts of imperfect kitten states and photon number detectors are analyzed in Sec. IV. In Sec. V, a protocol for the experimental implementation of the scheme based on a quantum frequency comb is proposed. Concluding remarks are provided in Sec. VI.

II. GENERAL MODEL FOR CAT STATE PRODUCTION WITH l -ADDED-AND- k -SUBTRACTED SQUEEZED VACUUM STATES

A. Schrödinger cat states

Optical Schrödinger cat states, i.e., the superposition of two coherent states with opposite phases, $|\beta\rangle$ and $|-\beta\rangle$, can be

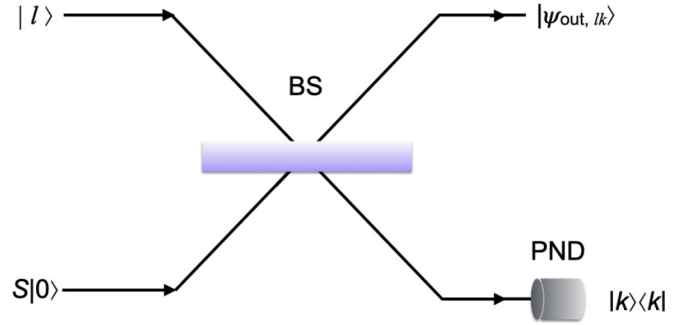


FIG. 1. Schematic diagram of Schrödinger cat state generation based on l -added-and- k -subtracted squeezed vacuum states BS: Beam splitter; PND: Photon number detector

written as [1]

$$|\psi_{\text{cat}}\rangle = N_{\pm}(|\beta\rangle \pm |-\beta\rangle), \quad (1)$$

where,

$$N_{\pm} = \frac{1}{\sqrt{2(1 \pm e^{-2|\beta|^2})}}, \quad (2)$$

$$|\beta\rangle = e^{-\frac{|\beta|^2}{2}} \sum_{n=0}^{\infty} \frac{\beta^n}{\sqrt{n!}} |n\rangle, \quad (3)$$

in which $|n\rangle$ is a Fock state. “+” and “−” represent even and odd Schrödinger cat states, respectively. N_{\pm} are the corresponding normalization constants. Substituting Eq. (3) to Eq. (1), it can be seen that only even (odd) photons are distributed in even (odd) cat states. To ensure two superposed coherent states are orthogonal, the overlap between $|\beta\rangle$ and $|-\beta\rangle$ should approach zero [7], i.e.,

$$\langle \beta | -\beta \rangle = e^{-|\beta|^2} \sum_{n=0}^{\infty} \frac{(-\beta^2)^n}{n!} = e^{-2|\beta|^2} \approx 0, \quad (4)$$

when $|\beta| \geq 2$.

B. General model of l -added-and- k -subtracted squeezed vacuum states

Similar to an even cat state, a squeezed vacuum state only contains even photon number distribution, which is written as [1,19],

$$\hat{S}(\xi)|0\rangle = \sum_{n=0}^{\infty} \alpha_{2n} |2n\rangle, \quad (5)$$

where

$$\alpha_{2n} = \frac{1}{\sqrt{\cosh \xi}} \frac{\sqrt{(2n)!} \tanh^n \xi}{2^n n!}, \quad (6)$$

and ξ is the squeezing parameter. Thus, a squeezed vacuum state is a high-fidelity ($F \geq 99\%$) approximation to the even kitten states ($|\beta| \leq 0.75$) [19]. Odd photon number distribution can be obtained if odd photons such as 1 or 3 are added or subtracted from a squeezed vacuum state. So it is an effective approach to generating Schrödinger kitten states. Here, we generalize the model to l -added-and- k -subtracted squeezed vacuum states as shown in Fig. 1. Such model is

a quantum linear system driven by multichannel multiphoton states [30–32]. The total input state of the system can be written as,

$$|\Psi_{\text{in}}\rangle = |l\rangle \otimes \sum_{n=0}^{\infty} \alpha_{2n} |2n\rangle. \quad (7)$$

According to tensor operation of quantum linear system driven by multichannel multiphoton states [30–32], the generated state at the output of the beam splitter can be derived as,

$$\begin{aligned} |\Psi_{\text{out}}\rangle &= \sum_{n=0}^{\infty} \frac{\alpha_{2n}}{\sqrt{\ell!(2n)!}} \sum_{i=0}^{\ell} \sum_{j=0}^{2n} \binom{\ell}{i} \binom{2n}{2n-j} \\ &\times \sqrt{(\ell+j-i)!(2n+i-j)!} \\ &(-1)^j T^{2n+\ell-i-j} R^{i+j} |\ell+j-i\rangle \otimes |2n+i-j\rangle, \end{aligned} \quad (8)$$

where, R^2 and T^2 are the reflectivity and transmittance of the beam splitter. When conditional measurement is conducted with a Fock state $|k\rangle$, we have

$$|\Psi_{\text{out}, lk}\rangle = \sum_{n=0}^{\infty} \gamma_{n, lk} |2n+l-k\rangle, \quad (9)$$

where,

$$\begin{aligned} \gamma_{n, lk} &= \frac{\alpha_{2n}}{\sqrt{\ell!(2n)!}} \sum_{j=\max(k-l, 0)}^{\min(k, 2n)} \binom{l}{l-k+j} \binom{2n}{2n-j} \\ &\sqrt{k!(2n+l-k)!} (-1)^j T^{2n+k-2j} R^{l-k+2j}. \end{aligned} \quad (10)$$

The density matrix of the heralded state in Eq. (9) is described as $\rho_{\text{out}, lk} = |\Psi_{\text{out}, lk}\rangle\langle\Psi_{\text{out}, lk}|$. The successful probability to obtain k photons on the conditional measurement is expressed as [33],

$$S(k) = \text{Tr}[\rho_{\text{out}, lk}], \quad (11)$$

which is normalized as $\sum_{k=0}^{\infty} S(k) = 1$ and $\rho_{\text{out}, lk}$ is the unnormalized density matrix.

The fidelity between two mixed states with density matrices ρ_1 and ρ_2 is generally defined as

$$F(\rho_1, \rho_2) = (\text{Tr}[(\sqrt{\rho_1}\rho_2\sqrt{\rho_1})^{\frac{1}{2}}])^2, \quad (12)$$

where, $\text{Tr}[\]$ denotes the trace of a matrix [34]. In the case of Schrödinger cat state generation, an ideal pure cat state $|\psi_{\text{cat}}\rangle$ is always used to calculate the fidelity. Thus, Eq. (12) can be rewritten as,

$$F(\rho_{\text{out}, lk}, \psi_{\text{cat}}) \triangleq \langle\psi_{\text{cat}}|\tilde{\rho}_{\text{out}, lk}|\psi_{\text{cat}}\rangle, \quad (13)$$

where $\tilde{\rho}_{\text{out}, lk}$ is the normalized density matrix of the heralded state shown in Eq. (9).

When $l-k$ is odd, an odd cat state is produced, while an even cat state is generated when $l-k$ is even. The case, $l=0$ and $k=1$, i.e., one-photon subtracted squeezed vacuum state, has become the standard approach to generating odd kitten states [13–16]. Here, we analyzed the performance of l -added-and- k -subtracted 5 dB (i.e., $\xi = 0.576$) squeezed vacuum states with different l and k . We change the reflectivity of

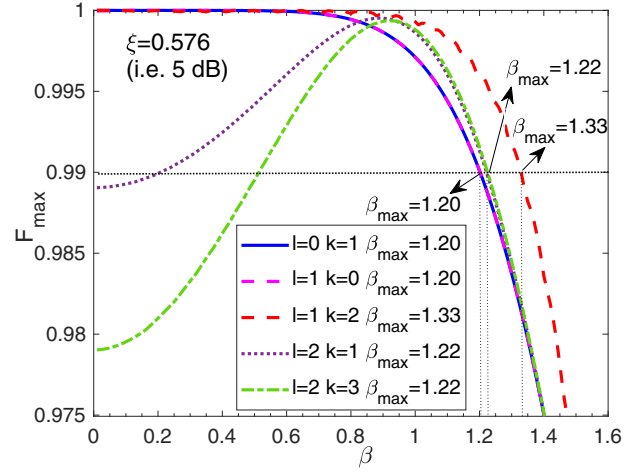


FIG. 2. Fidelity between an ideal odd cat state and the generated cat states from l -added-and- k -subtracted 5 dB squeezed vacuum states for different l and k .

the beam splitter and find the maximum fidelity between the generated cat state and an ideal cat state for different β . The variations of the fidelity with β are shown in Fig. 2, where β_{max} is taken as the maximum value of $|\beta|$ when $F = 99\%$. It is verified that the size of high-fidelity ($F \geq 99\%$) kitten states generated from one-photon subtracted squeezed vacuum state is limited as $|\beta| = 1.20$ [18,19], even though 5 dB squeezed vacuum state is utilized. In addition, the performance of one-photon subtracted squeezed vacuum state is verified to be similar to that of one-photon added squeezed vacuum state. Moreover, high-fidelity kitten states with $|\beta| > 1.20$ can be obtained in the higher-order photon manipulation schemes such as $l=1$ and $k=2$ as well as $l=2$ and $k=1$, which break the limit, $|\beta| = 1.20$ [18,19], of the standard approach with $l=0$ and $k=1$.

III. MODEL FOR LARGE-SIZE SCHRÖDINGER CAT STATE GENERATION

An approach to generating large-size Schrödinger cat states based on l -added-and- k -subtracted squeezed vacuum states is proposed as shown in Fig. 3. Two in-phase Schrödinger kitten states generated with l -added-and- k -subtracted squeezed vacuum states are combined on the third beam splitter (BS3). The total input state to BS3 is described as,

$$\begin{aligned} |\Psi_{\text{out}, l_1 k_1}^1\rangle \otimes |\Psi_{\text{out}, l_2 k_2}^2\rangle &= \sum_{n=0}^{\infty} \sum_{m=0}^{\infty} \gamma_{n, l_1 k_1}^1 \gamma_{m, l_2 k_2}^2 \\ &|2n+l_1-k_1\rangle_1 \otimes |2m+l_2-k_2\rangle_2, \end{aligned} \quad (14)$$

where, $\gamma_{n, l_1 k_1}^1$ and $\gamma_{m, l_2 k_2}^2$ have the same formats to $\gamma_{n, lk}$ in Eq. (10). The total input state is a linear combination of products $|2n+l_1-k_1\rangle_1 \otimes |2m+l_2-k_2\rangle_2$, where $n, m = 0, \dots, \infty$. According to the general theory in Refs. [30–32],

BS3 implements the following mapping:

$$\begin{aligned}
 & |2n + \ell_1 - k_1\rangle_1 \otimes |2m + \ell_2 - k_2\rangle_2 \\
 \rightarrow & \frac{1}{\sqrt{(2n + \ell_1 - k_1)!(2m + \ell_2 - k_2)!}} \sum_{j=0}^{2n+\ell_1-k_1} \sum_{l=0}^{2m+\ell_2-k_2} \binom{2n + \ell_1 - k_1}{j} \binom{2m + \ell_2 - k_2}{l} (-1)^l \\
 & T_3^{2m+\ell_2-k_2+j-l} R_3^{2n+\ell_1-k_1-j+l} \sqrt{(j+l)!(2n + \ell_1 - k_1 + 2m + \ell_2 - k_2 - j - l)!} \\
 & |j+l\rangle_1 |2n + \ell_1 - k_1 + 2m + \ell_2 - k_2 - j - l\rangle_2. \\
 = & \sum_{j=0}^{2n+\ell_1-k_1} \sum_{l=0}^{2m+\ell_2-k_2} \gamma_{n,m,j,l} |j+l\rangle_1 |2n + \ell_1 - k_1 + 2m + \ell_2 - k_2 - j - l\rangle_2,
 \end{aligned} \tag{15}$$

where

$$\gamma_{n,m,j,l} \triangleq \frac{(-1)^l T_3^{2m+\ell_2-k_2+j-l} R_3^{2n+\ell_1-k_1-j+l}}{\sqrt{(2n + \ell_1 - k_1)!(2m + \ell_2 - k_2)!}} \binom{2n + \ell_1 - k_1}{j} \binom{2m + \ell_2 - k_2}{l} \sqrt{(j+l)!(2n + \ell_1 - k_1 + 2m + \ell_2 - k_2 - j - l)!}. \tag{16}$$

Consequently, the final output state of BS3 is

$$|\Psi\rangle = \sum_{n=0}^{\infty} \sum_{m=0}^{\infty} \gamma_{n, \ell_1 k_1}^1 \gamma_{m, \ell_2 k_2}^2 \sum_{j=0}^{2n+\ell_1-k_1} \sum_{l=0}^{2m+\ell_2-k_2} \gamma_{n,m,j,l} |j+l\rangle_1 |2n + \ell_1 - k_1 + 2m + \ell_2 - k_2 - j - l\rangle_2. \tag{17}$$

When k photons are detected, the heralded output state is

$$|\Psi_k\rangle = \sum_{n=0}^{\infty} \sum_{m=0}^{\infty} \gamma_{n, \ell_1 k_1}^1 \gamma_{m, \ell_2 k_2}^2 \sum_{j=0}^{2n+\ell_1-k_1} \gamma_{n,m,j,k-j} |2n + \ell_1 - k_1 + 2m + \ell_2 - k_2 - k\rangle. \tag{18}$$

Therefore, odd (even) cats could be generated when $l_1 - k_1 + l_2 - k_2 - k$ is odd (even). In what follows, we will focus on the simplest case, $l_1 = l_2 = 0$, $k_1 = k_2 = 1$, and $k = 1$ by considering the experimental feasibility of the scheme.

A. Amplification of Schrödinger kitten states

As one-photon subtracted squeezed vacuum state is a standard approach to generating kitten states [13–16], which corresponds to the case of $l = 0$, $k = 1$ in Fig. 1, we investigate the amplification effect of the scheme shown in Fig. 3 when two unbalanced kitten states are inputs. Two unbalanced kitten states with amplitudes of $|\beta| = 1.11$ and $|\beta| = 1.06$ are generated from one-photon subtracted 3 dB squeezed vacuum states (corresponding to $\xi = 0.346$) via BS1 and BS2 with reflectivities of $R_1^2 = 0.05$ and $R_2^2 = 0.15$, respectively. Figures 4(a), 4(b) and 4(c) depict the photon number distribution and Wigner function of two input unbalanced kitten states and the amplified cat state when $R_3^2 = 0.49$. The features of odd photon number distribution in two input kitten states and the amplified state reveal that the cat parity is remained during the amplification. The fidelity of the input kitten states, BS3IN1 and BS3IN2, as well as the amplified state (BS3OUT) to an ideal odd cat state are represented by the dotted black line, dashed orange line, and dashed blue line in Fig. 4(d). It can be

seen that two input Schrödinger odd kitten states of $|\beta| = 1.11$ and $|\beta| = 1.06$ with $F = 99\%$ are amplified to a Schrödinger cat state of $|\beta| = 1.80$ and $F = 99\%$ with the same parity. In addition, the dotted magenta line in Fig. 4(d) implies the fidelity between the amplified cat state and a squeezed cat state, which indicates that the amplified cat state has a fidelity of $F = 99\%$ with a cat state of $|\beta| = 2.05$ squeezed by 1.39 dB. The amplification is also revealed by the Wigner function of the input kitten states and the generated state shown in the insets of Figs. 4(a)–4(c). Different from the Wigner function of the input kitten states, two positive Gaussian peaks related to the individual coherent state components can be clearly observed in the Wigner function of the amplified cat state shown in the inset of Fig. 4(c). The notable distance between two Gaussian peaks implying the large size of the generated cat state, which guarantees the distinguishability of two coherent-state components from the nonclassical interference fringes. Therefore, different from homodyne heralding scheme [21],

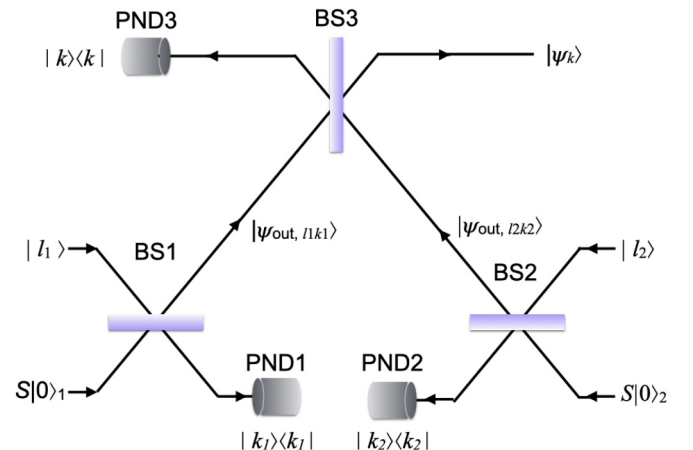


FIG. 3. Schematic diagram for large-size Schrödinger cat state generation BS: Beam splitter; PND: Photon number detector.

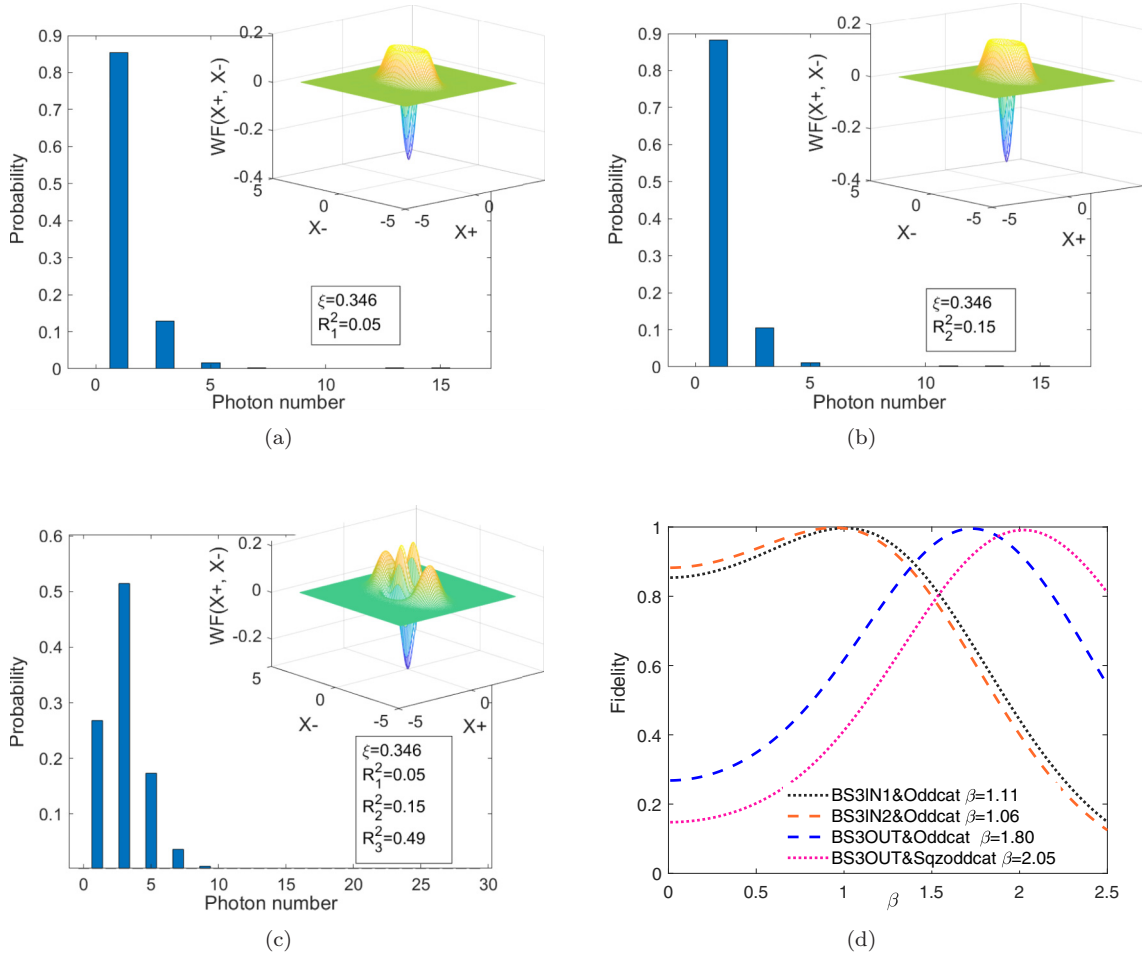


FIG. 4. Photon number distribution and Wigner function (insets) of two input kitten states (a) $|\beta| = 1.11$ (b) $|\beta| = 1.06$ as well as the amplified cat state (c) $|\beta| = 1.80$. (d) Comparison of fidelity variation for input states and output states and the corresponding $|\beta|$ when $F = 99\%$, dotted black line: fidelity between BS3IN1 and an ideal odd cat state, dashed orange line: fidelity between BS3IN2 and an ideal odd cat state, dashed blue line: fidelity between the amplified cat state BS3OUT and an ideal odd cat state, dotted magenta line: fidelity between the amplified cat state BS3OUT and an ideal cat state squeezed by 1.39 dB.

parity-preserving cat state amplification is realized in the scheme shown in Fig. 3.

B. Large-size Schrödinger cat state generation

The larger the amplitude of a cat state is, the bigger average photon number is generated since $\langle n \rangle = |\beta|^2$. Thus squeezed vacuum states with stronger squeezing level are required to generate cat states with $|\beta| \geq 2$. The variation of fidelity and the corresponding β of the amplified cat state with the squeezing parameter ξ of the squeezed vacuum states are shown in Fig. 5 when the reflectivities of three BSs are same to the case shown in Fig. 4, i.e., $R_1^2 = 0.05$, $R_2^2 = 0.15$ and $R_3^2 = 0.49$, which indicates that large-size cat states are available with stronger squeezed vacuum states, but the fidelity will decrease. Currently, 15 dB squeezed vacuum states have been generated for metrology [35]. To generate a cat state of $|\beta| \geq 2$ with sufficient fidelity, we select 5.91 dB squeezed vacuum states (corresponding to $\xi = 0.68$), which is easy to produce in the laboratory. To obtain large-size cat state with high-fidelity, numerical optimization was conducted by changing the reflectivities of BS1, BS2, and BS3 and finding the

maximum $|\beta|$ with a fidelity higher than 99%. Then reflectivities of BS1, BS2, and BS3 are optimized as $R_1^2 = 0.11$, $R_2^2 = 0.01$, and $R_3^2 = 0.505$, which result in two unbalanced kitten states with success probability of 4.49% and 0.47%. The photon number distribution, Wigner function, and the corresponding variation of fidelity for two unbalanced input kitten states and the generated cat state are shown in Figs. 6(a)–6(c), and 6(d). As is shown in Fig. 6(d), when two kitten states of $|\beta| = 1.39$ with $F = 97.17\%$ and $|\beta| = 1.52$ with $F = 95.47\%$ are input, a large-size Schrödinger cat state of $|\beta| = 2.51$ can be generated with the fidelity of $F = 97.30\%$. In this case, the success probability is 0.27%. The large size of the generated cat state is also revealed by the prominent distance between two distinguishable Gaussian peaks in the Wigner function shown in the inset of Fig. 6(c). The total success probability is around 5.7×10^{-7} , where we detect three photons in total. In general, the success probability is an exponential function of the number of total photons detected (not necessarily the number of photon detectors). In the experiments where three photons were detected to generate a cat state, the success probabilities were $\sim 10^{-9}$ with $|\beta| \approx 1.70$ in Ref. [25], and $\sim 10^{-7}$ with $|\beta| \approx 1.60$ in Ref. [36]. In

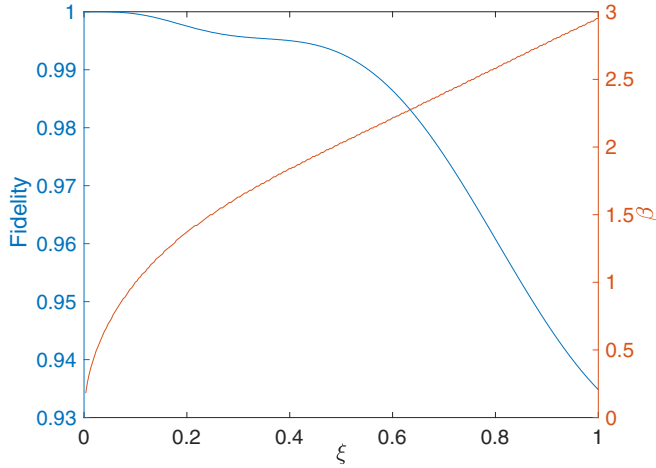


FIG. 5. Impact of squeezing parameter ξ of the input squeezed vacuum states on the fidelity F and the size of the amplified cat state $|\beta|$.

Ref. [21] where two photons were detected with the additional homodyne conditioning, the success probability was $\sim 10^{-8}$ with $|\beta| \approx 1.85$. Thus the success probability of our scheme is comparable with the existing experiments, while we expect the large-size Schrödinger cat state with $|\beta| \geq 2$. We also note that the experimental imperfections do not necessarily reduce the success probability while the imperfections significantly reduce the fidelity as we will see in the next section. Therefore, the proposed scheme in Fig. 3 provides an effective approach to generating large-size Schrödinger cat states with $|\beta| \geq 2$.

IV. MODEL WITH SYSTEM IMPERFECTIONS

A. Imperfections in the kitten states generation

When a Schrödinger kitten state is generated by subtracting one photon from a squeezed vacuum state, it is necessary to

$$\rho_{\text{out}} = \sum_{m,p=0}^{\infty} \sum_{n,q=0}^{\infty} \frac{a_{mn} b_{pq}}{\sqrt{m!n!p!q!}} \sum_{j_1=0}^m \sum_{i_1=0}^p \sum_{j_2=0}^n \sum_{i_2=0}^q \binom{m}{j_1} \binom{p}{i_1} \binom{n}{j_2} \binom{q}{i_2} (-1)^{i_1+i_2} T_3^{p+q+j_1+j_2-i_1-i_2} R_3^{m+n+i_1+i_2-j_1-j_2} \sqrt{(j_1+i_1)!(j_2+i_2)!(m+p-j_1-i_1)!(n+q-j_2-i_2)!} |j_1+i_1\rangle_1 |m+p-j_1-i_1\rangle_2 |n+q-j_2-i_2\rangle_1 |j_2+i_2\rangle_2. \quad (21)$$

If we conduct conditional measurement by a Fock state $|k\rangle$, then the unnormalized heralded state is

$$\rho_{\text{out},k} \triangleq \langle k | \rho_{\text{out}} | k \rangle = \sum_{m=0}^{\infty} \sum_{p=\max(0,k-m)}^{\infty} \sum_{n=0}^{\infty} \sum_{q=\max(0,k-n)}^{\infty} \frac{a_{mn} b_{pq} k!}{\sqrt{m!n!p!q!}} \sqrt{(m+p-k)!(n+q-k)!} \times \sum_{j_1=\max(0,k-p)}^{\min(m,k)} \sum_{j_2=\max(0,k-q)}^{\min(n,k)} \binom{m}{j_1} \binom{p}{k-j_1} \binom{n}{j_2} \binom{q}{k-j_2} (-1)^{j_1+j_2} T_3^{p+q+2(j_1+j_2-k)} \times R_3^{m+n-2(j_1+j_2-k)} |m+p-k\rangle \langle n+q-k|. \quad (22)$$

Similar to Eq. (11), we can get the success probability to obtain k photons in the conditional measurement as $S_{\text{amp}}(k) = \text{Tr}[\rho_{\text{out},k}]$.

consider various imperfections such as impurity of the input squeezed vacuum state, dark counts, detection efficiency, and the non-photon-number-resolving ability of the single photon detector, and so on. The impacts and physical mechanism of all these imperfections are analyzed in detail in Ref. [37]. While the development of photon-number-resolving single-photon detectors such as superconducting transition-edge sensors (TESs) provides single-photon detectors with quantum detection efficiency as high as 0.98 and negligible dark counts [38], which significantly facilitates Schrödinger cat state generation based on photon subtraction. Therefore, we can use TESs as the PNDs in Fig. 3 and just consider the impurity of the squeezed vacuum states (equivalent to the loss) and the detection efficiency of the photon-number-resolving single-photon detectors here. According to the Schrödinger kitten state model reported in Ref. [37], the generated kitten states from BS1 and BS2 are mixed states, described as ρ_1 and ρ_2 , which are functions of the squeezing parameter ξ , the loss of the squeezed vacuum states, γ_{sqzvac} , reflectivities of BS1 and BS2, R_1^2 and R_2^2 , as well as the detection efficiency of the photon-number-resolving PND, η_{PND} . A general model involving experimental imperfections for the kitten state amplification scheme is developed. Two input kitten states with experimental imperfections ρ_1 and ρ_2 , can be written as

$$\rho_1 = \sum_{m,n=0}^{\infty} a_{mn} |m\rangle \langle n|, \quad \rho_2 = \sum_{p,q=0}^{\infty} b_{pq} |p\rangle \langle q|, \quad (19)$$

where $a_{nm} = a_{mn}^*$, and $b_{qp} = b_{pq}^*$. a_{mn}^* and b_{pq}^* are conjugates of a_{mn} and b_{pq} , respectively. Then the input state to BS3 is described as,

$$\rho_{\text{in}} = \rho_1 \otimes \rho_2 = \sum_{m,n=0}^{\infty} \sum_{p,q=0}^{\infty} a_{mn} b_{pq} |mp\rangle \langle qn|. \quad (20)$$

The output from BS3 is derived as

B. Detection inefficiency of PND at BS3

As analyzed in Ref. [37], when k photons are actually subtracted in the conditional measurement, m ($m \leq k$) photons

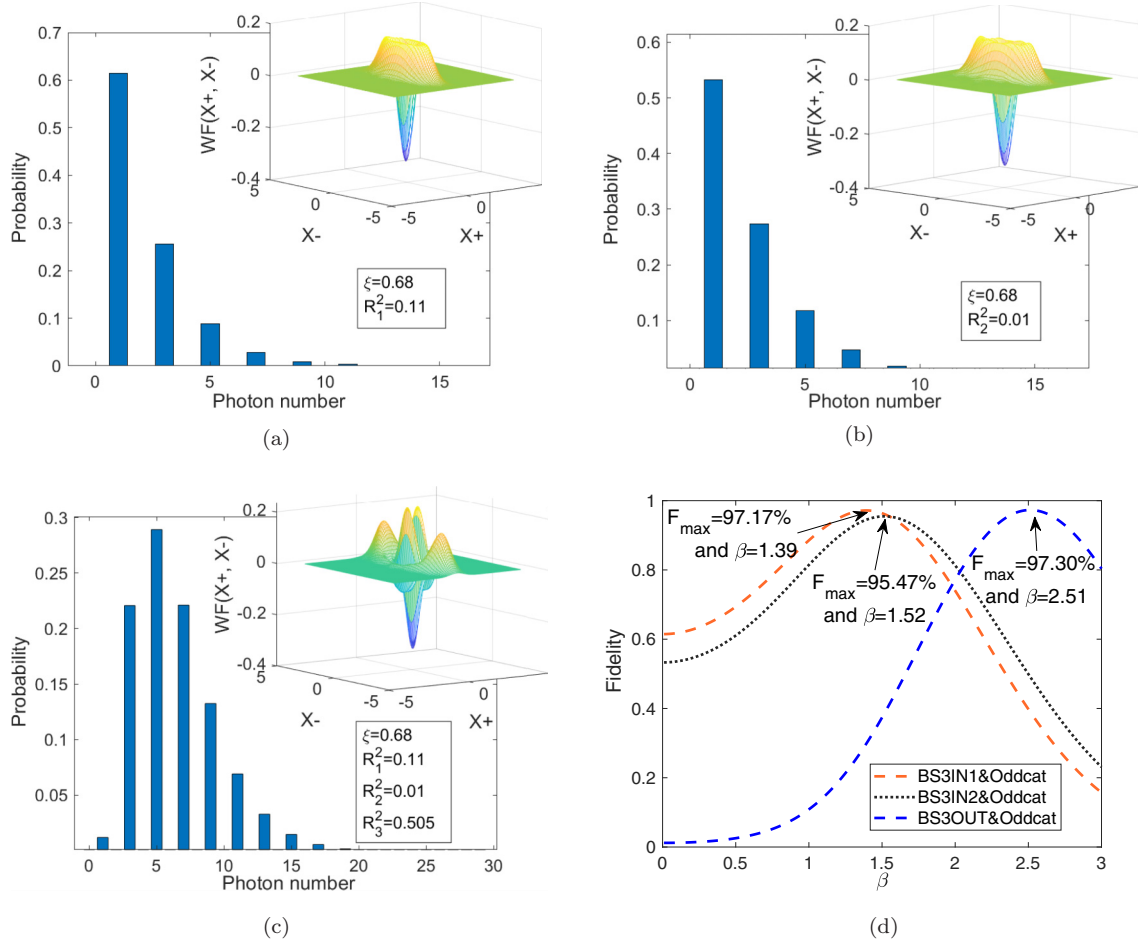


FIG. 6. Photon number distribution and Wigner function (insets) of two input kitten states with (a) $|\beta| = 1.39$, (b) $|\beta| = 1.52$, and the amplified cat state with (c) $|\beta| = 2.51$. (d) Corresponding curves of fidelity varying with $|\beta|$ dashed orange line: fidelity between BS3IN1 and an ideal odd cat state, dotted black line: fidelity between BS3IN2 and an ideal odd cat state, dotted blue line: fidelity between the amplified cat state BS3OUT and an ideal odd cat state.

may be detected due to the impact of detection inefficiency of PND. Assume that m photons are detected by the photon-number detector with a detection efficiency of η_{PND} , the density matrix of the output state is

$$\rho_{\text{IMPND}}(m) = \sum_{k=1}^{\infty} Q(k|m) \rho_{\text{out},k}, \quad (23)$$

where $Q(k|m)$ is the probability that m photons are detected while k photons are actually subtracted and $\rho_{\text{out},k}$ is the density matrix when k photons are actually subtracted as described in Eq. (22). $Q(k|m)$ can be written as

$$Q(k|m) = \frac{P(m|k)S_{\text{amp}}(k)}{\sum_i P(m|i)S_{\text{amp}}(i)}, \quad (24)$$

where $S_{\text{amp}}(k)$ is the probability that k photons have been subtracted and $P(m|k)$ is the probability that m photons have been detected when k photon are actually subtracted, which is expressed as

$$P(m|k) = \frac{k! \eta_{\text{PND}}^m (1 - \eta_{\text{PND}})^{k-m}}{m!(k-m)!}, \quad (25)$$

in which η_{PND} is the quantum efficiency of the photon-number-resolving detector [39].

C. Simulation results

As highly efficient single-photon detectors such as TESs with photon-number-resolving ability and negligible dark counts are available [38], we can replace PNDs in the cat state amplification scheme with TESs. Without losing the generality, we take $\eta_{\text{PND}} = 0.95$ and $\gamma_{\text{sqzvac}} = 0.01$. The photon number distribution and Wigner functions (WF) of the amplified cat state heralded with a perfect and imperfect PND3 are analyzed in the case of $\xi = 0.68$ (i.e., 5.91 dB squeezed vacuum states). Comparing with the photon number distribution of the amplified cat state heralded with an ideal PND3 shown in Fig. 7(a), $P(n)$ with $n = 2, 4, 6, \dots$ in the photon number distribution of the amplified cat state heralded with an imperfect PND3 are increased as shown in Fig. 7(b). At the same time, significant negativities in the Wigner function are kept in both cases as shown in Figs. 7(c) and 7(d), which indicate the nonclassicality of the generated state. Furthermore, the negativity in the origin of the Wigner function, $\text{WF}(0,0)$, in the generated state also shows the odd parity of the amplified

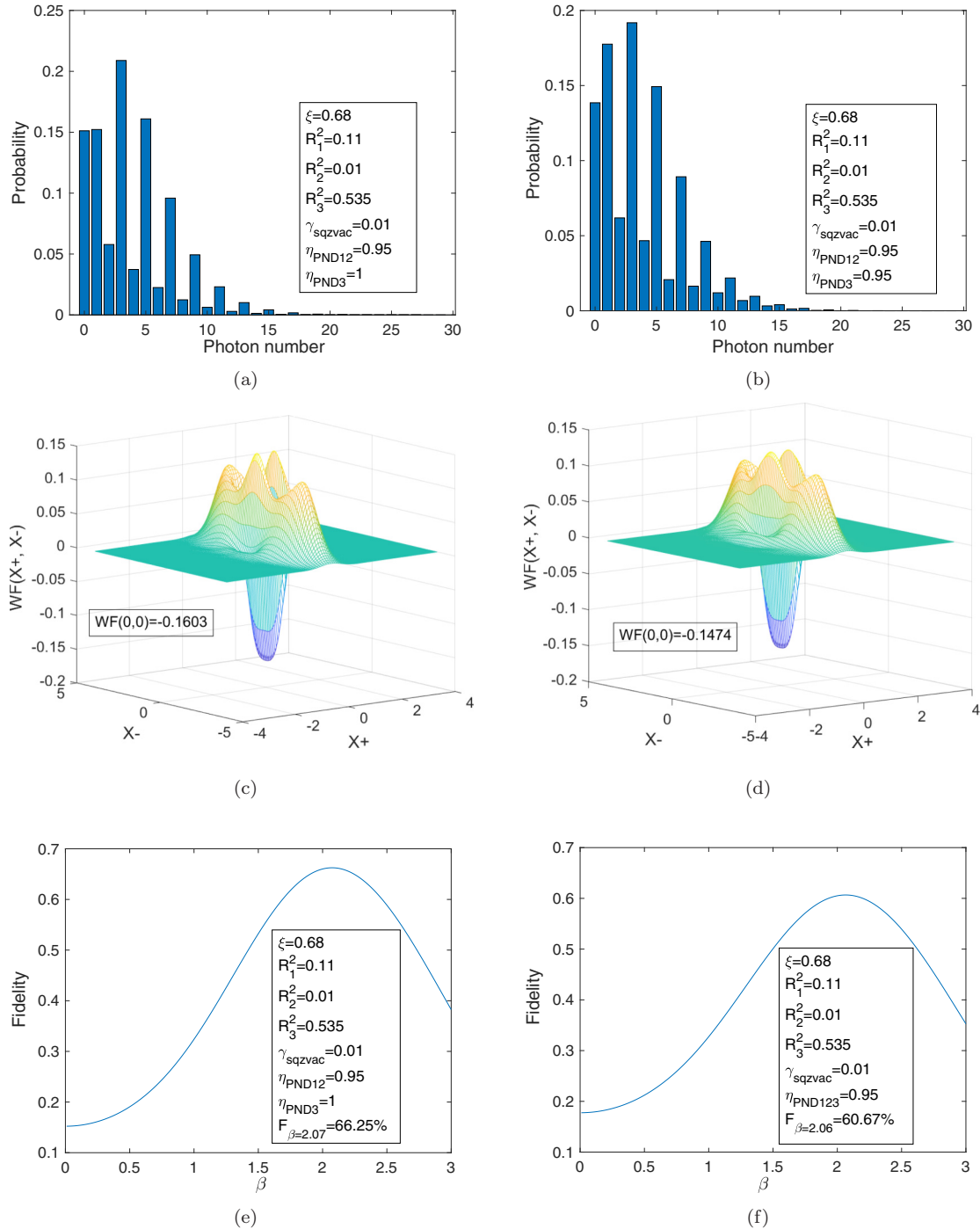


FIG. 7. Amplified cat states heralded with a perfect (left) and imperfect (right) PND3. (a) and (b) Photon number distribution; (c) and (d) Wigner function. (e) and (f) Fidelity variation with the amplitude of an ideal cat state.

state, which verifies the odd parity preservation of the scheme. Therefore, different from the parity change in Ref. [21], the input odd kitten states are amplified to an odd cat state in the scheme we proposed. Figures 7(e) and 7(f) imply that the amplified cat state of $|\beta| = 2.07$ and $F = 66.25\%$ as well as $|\beta| = 2.06$ and $F = 60.67\%$ (the fidelity is comparable with $F = 59.29\%$ reported in Ref. [21] when the same format of fidelity is employed) can be generated with a perfect and imperfect PND3. The success probability is 1.08%. It is noted that the generated cat state is sensitive to the loss of the

squeezed vacuum states and the detection efficiency of PND3. With the best TES (i.e., $\eta_{\text{PND}} = 0.98$) cat states with larger size and higher fidelity can be predicted.

V. PROPOSAL OF EXPERIMENTAL REALIZATION BASED ON A QUANTUM FREQUENCY COMB

Similar to homodyne heralding cat state amplification scheme [21], two kitten states are required to obtain a large-size cat state in our proposal. Such kitten states are

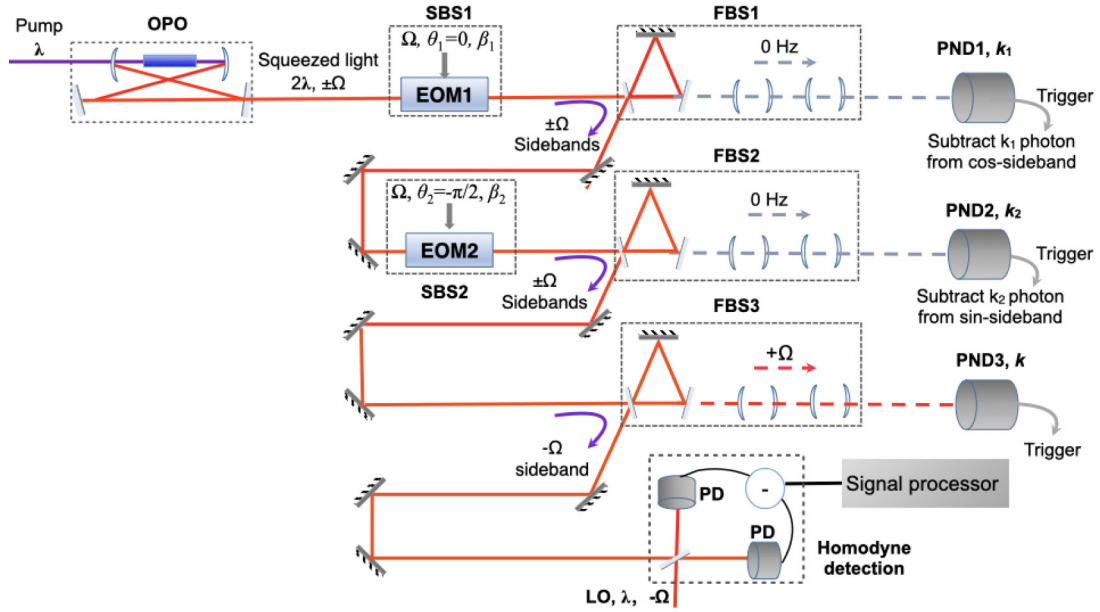


FIG. 8. Quantum-frequency-comb-based large-size cat state generation scheme OPO: Optica parametric oscillator; SBS: Sideband beam splitter; EOM: Electro-optic modulator; FBS: Frequency beam splitter; PND: Photon-number detector; LO: Local oscillator; PD: Photodetector.

traditionally generated with one-photon subtracted squeezed vacuum states from an optical parametric oscillator (OPO). Thus, two OPOs are required, which makes the system quite complicated. To simplify the experimental setup, we propose a quantum-frequency-comb-based protocol to realize the scheme shown in Fig. 3 by extending the sideband Schrödinger cat state generation scheme reported in Ref. [17]. As a specific example, we just focus on the case discussed in the previous part, i.e., $l_1 = l_2 = 0$, $k_1 = k_2 = 1$, and $k = 1$ in Fig. 3, which can be realized by the quantum-frequency-comb-based protocol shown in Fig. 8. It is worth noting that arbitrary-number-photon subtraction can be realized, i.e., k_1 , k_2 , and k could be arbitrary integers.

A series of entangled photon pairs at $\omega_0 \pm n\Omega$ ($n = 1, 2, 3 \dots$), can be generated by an OPO or optical parametric amplifier, which form a comblike shape [40–42]. For simplicity, we set the baseband at $\omega_0 = 0$ Hz and then the sidebands can be described as $\pm\Omega$. Different from the quantum frequency comb used in quantum teleportation in Ref. [43], the resonant frequency of the OPO in Fig. 8 is set at the sidebands, i.e. $\pm\Omega$, rather than the baseband, which provides a vacuum state at 0 Hz due to the antiresonance. A double sideband (DBS) mode is defined as $(e^{i\theta}\hat{a}_{+\Omega} + e^{-i\theta}\hat{a}_{-\Omega})/\sqrt{2}$, where $\hat{a}_{\pm\Omega}$ is the annihilation operator at frequency $\pm\Omega$ and θ is an arbitrary phase. A DSB mode can be decomposed into two quadrature-phase components, cos sideband and sin sideband [42],

$$\hat{a}_{\Omega}^{\cos} = \frac{\hat{a}_{+\Omega} + \hat{a}_{-\Omega}}{\sqrt{2}} \quad (26)$$

$$\hat{a}_{\Omega}^{\sin} = \frac{\hat{a}_{+\Omega} - \hat{a}_{-\Omega}}{\sqrt{2}i}, \quad (27)$$

corresponding to $\theta = 0$ and $\theta = -\pi/2$, respectively, from which independent squeezed states are available. Schrödinger

kitten states can be obtained by subtracting one photon from both cos sideband and sin sideband [17], in which one-photon subtraction from the DBS is realized through a unit composed of an electro-optic modulator (EOM), an optical cavity and a PND. The EOM plays the role of sideband beam splitter (SBS) via phase modulation. After EOM1, the signal from the OPO, \hat{a}_{ω} , becomes

$$\hat{a}_{\omega}^{\text{mod}} \sim \sqrt{1 - \frac{\Gamma^2}{2}}\hat{a}_{\omega} + \frac{\Gamma}{2}(e^{i\theta}\hat{a}_{\omega+\Omega} + e^{-i\theta}\hat{a}_{\omega-\Omega}), \quad (28)$$

where $\Gamma \ll 1$ indicates the modulation depth and θ is determined by the modulation phase [17]. While $T^2 = 1 - \frac{\Gamma^2}{2}$ is equivalent to the transmittance of a beam splitter. The optical cavity following the EOM plays as a frequency beam splitter (FBS) separating and filtering different frequency components by transmitting all baseband and reflecting all sideband signals. Thus the signal from the PND works as a trigger, which heralds [17],

$$\text{trigger} \langle 1 | \sim_{\text{sig}} \langle 0 | \left(\hat{a}_0 + \frac{\Gamma}{\sqrt{2}} \frac{e^{i\theta}\hat{a}_{+\Omega} + e^{-i\theta}\hat{a}_{-\Omega}}{\sqrt{2}} \right). \quad (29)$$

Note that Eq. (29) is unnormalized and valid only under the condition of $\Gamma \ll 1$. As a vacuum state at 0 Hz is provided due to the antiresonance of the OPO, the trigger shown in Eq. (29) will subtract a photon from the DSB mode with the phase θ . The cos sideband and sin sideband can be accessed by selecting the parameters of two EOMs,

$$\theta_1 = 0, \quad T_1^2 = 1 - \frac{\Gamma_1^2}{2} \quad (30)$$

$$\theta_2 = -\frac{\pi}{2}, \quad T_2^2 = 1 - \frac{\Gamma_2^2}{2}, \quad (31)$$

in which T_i^2 ($i = 1$ and 2) determined by the modulation depth Γ_i ($i = 1$ and 2) of two EOMs in Fig. 8 correspond to the

transmittance of BS1 and BS2 shown in Fig. 3. T_i can be adjusted by tuning the modulation depth of EOMs. Therefore, two unbalanced kitten states in both cos sideband and sin sideband are generated before entering into FBS3. Different from FBS1 and FBS2, FBS3 is designed as a beam splitter of the DBS by separating component $+\Omega$ from $-\Omega$ since we have,

$$\hat{a}_{+\Omega} = \frac{\hat{a}_{\Omega}^{\cos} + i\hat{a}_{\Omega}^{\sin}}{\sqrt{2}}, \quad (32)$$

$$\hat{a}_{-\Omega} = \frac{\hat{a}_{\Omega}^{\cos} - i\hat{a}_{\Omega}^{\sin}}{\sqrt{2}}. \quad (33)$$

A trigger signal at $+\Omega$ is generated from PND3. The function of BS3 with $T_3^2 = \frac{1}{2}$ in Fig. 3 is realized by shifting the local oscillator in the homodyne detection to the frequency of $-\Omega$. If PND3 is replaced with homodyne detection, the cat amplification scheme based on homodyne heralding reported in Ref. [21] could be realized. By designing FBS3 to reflect partial $+\Omega$ and transmit a part of $-\Omega$, T_3 is adjustable to meet the requirement of cat amplification discussed in Secs. III and IV. Thus, the implementation of scheme $l_1 = l_2 = 0$, $k_1 = k_2 = 1$, and $k = 1$ shown in Fig. 3 is successfully achieved with a quantum frequency comb.

In addition, if other sidebands, such as $\pm n\Omega$ in the frequency comb are used, multiple large-size cat states are available. It is also possible to amplify the cat state further by an iterative structure. Therefore, the quantum-frequency-comb-based protocol provides a different approach to producing real coherent-state superposed quantum light source for quantum information processing. We also note that the imperfection analysis developed in Sec. IV is applied to the quantum frequency comb realization, where the finite

transmission of the frequency beam splitter is accumulated to the detection efficiency of the corresponding PND.

VI. CONCLUSION

In conclusion, a scheme to amplify Schrödinger kitten states based on linear operation and conditional measurement with photon number detection is proposed and analyzed. According to the general model of l -added-and- k -subtracted squeezed vacuum states developed based on tensor operation, the generated kitten states with $l = 1$ and $k = 2$ as well as $l = 2$ and $k = 1$ break the limit of $|\beta| = 1.20$ produced in the standard way, i.e., $l = 0$ and $k = 1$. Combining two kitten states and conducting conditional measurement via photon number detection, Schrödinger cat states with $|\beta| > 2$ are predicted in both theory and practice. A protocol for experimental implementation based on a quantum frequency comb is proposed. Multiple large-size Schrödinger cat states are possible to be generated by taking full advantages of the sidebands in a quantum frequency comb, which offers a new way of producing large-scale superposed coherent states to meet the demanding requirements of continuous-variable quantum computation and quantum communication.

ACKNOWLEDGMENTS

This work was supported by National Natural Science Foundation of China under Grant No. 61903316 and 6217023269, Shenzhen Fundamental Research Fund under the Grant No. JCYJ20190813165207290, the Hong Kong Research Grant Council (RGC) (Grants No. 15203619, No. 15208418, and No. 15506619), the Australian Research Council Centre of Excellence for Quantum Computation and Communication Technology (Project No. CE170100012), and the Optical Communication Core Chip Research Platform.

-
- [1] M. Dakna, T. Anhut, T. Opatrny, L. Knöll, and D. G. Welsch, Generation Schrödinger-cat-like states by means of conditional measurements on a beam splitter, *Phys. Rev. A* **55**, 3184 (1997).
 - [2] H. Jeong, W. Son, M. S. Kim, D. Ahn, and Č. Brukner, Quantum nonlocality test for continuous-variable states with dichotomic observables, *Phys. Rev. A* **67**, 012106 (2003).
 - [3] N. Sangouard, C. Simon, N. Gisin, J. Laurat, R. Tualle-Brouri, and P. Grangier, Quantum repeaters with entangled coherent states, *J. Opt. Soc. Am. B* **27**, A137 (2010).
 - [4] J. B. Brask, I. Rigas, E. S. Polzik, U. L. Andersen, and A. S. Sørensen, Hybrid Long-Distance Entanglement Distribution Protocol, *Phys. Rev. Lett.* **105**, 160501 (2010).
 - [5] J. S. Neergaard-Nielsen, Y. Eto, C. W. Lee, H. Jeong, and M. Sasaki, Quantum tele-amplification with a continuous variable superposition state, *Nature Photon.* **7**, 439 (2013).
 - [6] P. T. Cochrane, G. J. Milburn, and W. J. Munro, Macroscopically distinct quantum-superposition states as a bosonic code for amplitude damping, *Phys. Rev. A* **59**, 2631 (1999).
 - [7] T. C. Ralph, A. Gilchrist, and G. J. Milburn, Quantum computation with optical coherent states, *Phys. Rev. A* **68**, 042319 (2003).
 - [8] J. Hastrup, J. S. Neergaard-Nielsen, and U. L. Andersen, Deterministic generation of a four-component optical cat state, *Opt. Lett.* **45**, 640 (2020).
 - [9] A. P. Lund, T. C. Ralph, and H. L. Haselgrove, Fault-Tolerant Linear Optical Quantum Computing with Small-Amplitude Coherent States, *Phys. Rev. Lett.* **100**, 030503 (2008).
 - [10] A. Gilchrist, K. Nemoto, W. Munro, T. Ralph, S. Glancy, S. Braunstein, and G. Milburn, Schrödinger cats and their power for quantum information processing, *J. Opt. B* **6**, S828 (2004).
 - [11] W. J. Munro, K. Nemoto, G. J. Milburn, and S. L. Braunstein, Weak-force detection with superposed coherent states, *Phys. Rev. A* **66**, 023819 (2002).
 - [12] J. Joo, William J. Munro, and T. P. Spiller, Quantum Metrology with Entangled Coherent States, *Phys. Rev. Lett.* **107**, 083601 (2011).
 - [13] A. Ourjoumtsev, R. Tualle-Brouri, J. Laurat, and P. Grangier, Generating optical Schrödinger kittens for quantum information processing, *Science* **312**, 83 (2006).
 - [14] J. S. Neergaard-Nielsen, B. Melholt Nielsen, C. Hettich, K. Mølmer, and E. S. Polzik, Generation of a Superposition of Odd Photon Number States for Quantum Information Networks, *Phys. Rev. Lett.* **97**, 083604 (2006).

- [15] N. Namekata, Y. Takahashi, G. Fujii, D. Fukuda, S. Kurimura, and S. Inoue, Non-Gaussian operation based on photon subtraction using a photon-number-resolving detector at a telecommunications wavelength, *Nature Photon.* **4**, 655 (2010).
- [16] K. Wakui, H. Takahashi, A. Furusawa, and M. Sasaki, Photon subtracted squeezed states generated with periodically poled KTiOPO₄, *Opt. Express* **15**, 3568 (2007).
- [17] T. Serikawa, J. Yoshikawa, S. Takeda, H. Yonezawa, T. C. Ralph, E. H. Huntington, and A. Furusawa, Generation of a Cat State in an Optical Sideband, *Phys. Rev. Lett.* **121**, 143602 (2018).
- [18] A. P. Lund, H. Jeong, T. C. Ralph, and M. S. Kim, Conditional production of superpositions of coherent states with inefficient photon detection, *Phys. Rev. A* **70**, 020101(R) (2004).
- [19] A. M. Branczyk and T. C. Ralph, Teleportation using squeezed single photons, *Phys. Rev. A* **78**, 052304 (2008).
- [20] A. Ourjoumtsev, H. Jeong, R. Tualle-Brouri, and P. Grangier, Generation of optical Schrödinger cats from photon number states, *Nature (London)* **448**, 784 (2007).
- [21] D. V. Sychev, A. E. Ulanov, A. A. Pushkina, M. W. Richards, I. A. Fedorov, and A. I. Lvovsky, Enlargement of optical Schrödinger's cat states, *Nature Photon.* **11**, 379 (2017).
- [22] H. Takahashi, K. Wakui, S. Suzuki, M. Takeoka, K. Hayasaka, A. Furusawa, and M. Sasaki, Generation of Large-Amplitude Coherent-State Superposition via Ancilla-Assisted Photon Subtraction, *Phys. Rev. Lett.* **101**, 233605 (2008).
- [23] M. Takeoka, H. Takahashi and M. Sasaki, Large-amplitude coherent-state superposition generated by a time-separated two-photon subtraction from a continuous-wave squeezed vacuum, *Phys. Rev. A* **77**, 062315 (2008).
- [24] A. E. B. Nielsen, and K. Molmer, Transforming squeezed light into a large-amplitude coherent-state superposition, *Phys. Rev. A* **76**, 043840 (2007).
- [25] T. Gerrits, S. Glancy, T. S. Clement, B. Calkins, A. E. Lita, A. J. Miller, A. L. Migdall, S. Woo Nam, R. P. Mirin, and E. Knill, Generation of optical coherent-state superposition by number-resolved photon subtraction from the squeezed vacuum, *Phys. Rev. A* **82**, 031802(R) (2010).
- [26] A. Laghaout, J. S. Neergaard-Nielsen, I. Rigas, C. Kragh, A. Tipsmark, and U. L. Andersen, Amplification of realistic Schrödinger-cat-state-like states by homodyne heralding, *Phys. Rev. A* **87**, 043826 (2013).
- [27] K. Takase, J. Yoshikawa, W. Asavanant, M. Endo, and A. Furusawa, Generation of optical Schrödinger cat states by general photon subtraction, *Phys. Rev. A* **103**, 013710 (2021).
- [28] M. Eaton, R. Nehra, and O. Pfister, Non-Gaussian and Gottesman-Kitaev-Preskill state preparation by photon catalysis, *New J. Phys.* **21**, 113034 (2019).
- [29] E. V. Mikheev, A. S. Pugin, D. A. Kuts, S. A. Podoshvedov, and N. Ba An, Efficient production of large-size optical Schrödinger cat states, *Sci. Rep.* **9**, 14301 (2019).
- [30] G. Zhang, and M. James, On the response of quantum linear systems to single photon input fields, *IEEE Trans. Autom. Control* **58**, 1221 (2013).
- [31] G. Zhang, Analysis of quantum linear systems' response to multi-photon states, *Automatica* **50**, 442 (2014).
- [32] G. Zhang, Dynamical analysis of quantum linear systems driven by multi-channel multi-photon states, *Automatica* **83**, 186 (2017).
- [33] M. Ban, Photon statistics of conditional output states of lossless beam splitter, *J. Mod. Opt.* **43**, 1281 (1996).
- [34] R. Jozsa, Fidelity for mixed quantum states, *J. Mod. Opt.* **41**, 2315 (1994).
- [35] H. Vahlbruch, M. Mehmet, K. Danzmann, and R. Schnabel, Detection of 15 dB Squeezed States of Light and their Application for the Absolute Calibration of Photoelectric Quantum Efficiency, *Phys. Rev. Lett.* **117**, 110801 (2016).
- [36] M. Yukawa, K. Miyata, T. Mizuta, H. Yonezawa, P. Marek, R. Filip, and A. Furusawa, Generating superposition of up-to three photons for continuous variable quantum information processing, *Opt. Express* **21**, 5529 (2013).
- [37] H. Song, K. B. Kuntz, and E. H. Huntington, Limitations on the quantum non-Gaussian characteristic of Schrödinger kitten state generation, *New J. Phys.* **15**, 023042 (2013).
- [38] D. Fukuda, G. Fujii, T. Numata, K. Amemiya, A. Yoshizawa, H. Tsuchida, H. Fujino, H. Ishii, T. Itatani, S. Inour, and T. Zama, Titanium-based transition-edge photon number resolving detector with 98% detection efficiency with index-matched small-gap fiber coupling, *Opt. Express* **19**, 870 (2011).
- [39] H. Lee, U. Yurtsever, P. Kok, G. M. Hockney, C. H. Adami, S. L. Braunstein and J. Dowling, Towards photostatistics from photon-number discriminating detectors, *J. Mod. Opt.* **51**, 1517 (2004).
- [40] M. Kues, C. Reimer, J. M. Lukens, W. J. Munro, A. M. Weiner, D. J. Moss, and R. Morandotti, Quantum optical microcombs, *Nature Photon.* **13**, 170 (2019).
- [41] G. Maltese, M. I. Amanti, F. Appas, G. Sinnl, A. Lemaître, P. Milman, F. Baboux, and S. Ducci, Generation and symmetry control of quantum frequency combs, *npj Quantum Inf.* **6**, 13 (2020).
- [42] S. Shi, Y. Wang, L. Tian, J. Wang, Xiao. Sun, and Y. Zheng, Observation of a comb of squeezed states with a strong squeezing factor by a bichromatic local oscillator, *Opt. Lett.* **45**, 2419 (2020).
- [43] H. Song, H. Yonezawa, K. B. Kuntz, M. Heurs, and E. H. Huntington, Quantum teleportation in space and frequency using entangled pairs of photons from a frequency comb, *Phys. Rev. A* **90**, 042337 (2014).